REAL-TIME BLOCK FLOW TRACKING OF ATRIAL SEPTAL DEFECT MOTION IN 4D CARDIAC ULTRASOUND

Marius George Linguraru[1], Alexandre Kabla[1], Nikolay V. Vasilyev[2], Pedro J. del Nido[2], Robert D. Howe[1]

[1]Division of Engineering and Applied Sciences, Harvard University, Cambridge, MA, USA
[2]Department of Cardiac Surgery, Children's Hospital, Harvard Medical School, Boston, MA, USA

ABSTRACT

Real-time cardiac ultrasound allows monitoring the heart motion during intracardiac beating heart procedures. Our application assists atrial septal defect (ASD) closure techniques using real-time 3D ultrasound guidance. One major image processing challenge is the processing of information at high frame rate. We present an optimized block flow technique, which combines the probability-based velocity computation for an entire block with template matching. We propose adapted similarity constraints both from frame to frame, to conserve energy, and globally, to minimize errors. We show tracking results on eight in-vivo 4D datasets acquired from porcine beating-heart procedures. Computing velocity at the block level with an optimized scheme, our technique tracks ASD motion at 41 frames/s. We analyze the errors of motion estimation and retrieve the cardiac cycle in ungated images.

INDEX TERMS: 3D echocardiography, atrial septal defect, block flow, motion tracking, real-time.

1. INTRODUCTION

Real-time cardiac ultrasound (US) allows monitoring the heart motion during intracardiac beating heart procedures. Amongst the congenital heart malformations, secundum-type atrial septal defects (ASD) have been reported to account for up to 15% of cases [1]. ASD represent openings in the septum between the atria, which decrease the efficiency of heart pumping. Pediatric ASD closure studies using rigid instruments showed the feasibility of the procedures and highlighted their limitations [4,8]. Reliable visualization of structures within the heart remains a major challenge to successful beating-heart surgical interventions [3]. A 3D image of an ASD and its position in the heart is shown in Figure 1.

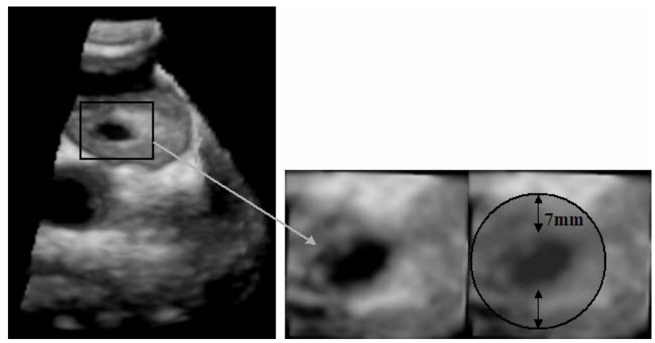

Figure 1: 3D US image of a porcine beating-heart with ASD. The US probe is placed on the exterior wall of the right atrium and pointed towards the left atrium. The image on the left shows the entire 3D US volume, while on the right we present a magnified view of the ASD. The patch must cover the entire ASD surface.

We previously introduced the basic concepts of a block flow technique to guide the correct placement of the patch over the ASD surface. A modified block flow algorithm is presented in Section 2 [5]. Our previous results showed excellent robustness for tracking ASD, but computational aspects of the presented implementation were impeding the real-time use of the application. The current streaming speed of commercial US machines is of 25 frames/s. Hence, a real-time US image-guided application would desirably achieve approximately 25 Hz processing speed.

2. METHOD

The block flow algorithm combines the velocity computation from optical flow for an entire block with template matching [5]. An absolute reference block *absref* is defined in the first frame of the 4D US sequence, which contains the ASD. In subsequent frames, the updated reference is *ref* and the target block *tar*. We normalize the voxel values as below, where *newref* imbeds both a measure of template/golden standard (*absref*) and updated reference (*ref*).

$$\overline{ref} = ref / \mu_{ref}; \ \overline{absref} = absref / \mu_{absref}; \ \overline{tar} = tar / \mu_{tar};$$

$$\overline{newref} = \left(\overline{ref} + \overline{absref}\right)/2;$$

The velocity or displacement of the block V_b is computed as a probability distribution function R, where n is the number of voxels in the 3D block and md the maximum displacement or search space [2,7]. The energy function E accounts for both the Rayleigh distribution of the noise model and logarithmic compression in US images.

$$E(\overline{newref}, \overline{tar}) = \frac{1}{n}\sum_i \left[\ln \overline{newref}_i - \ln \overline{tar}_i - \ln\left(e^{2\left(\ln \overline{newref}_i - \ln \overline{tar}_i\right)} + 1\right)\right];$$

$$R(u,v,w) = \frac{1}{\tau}\left(\exp\left(-\frac{E(\overline{newref}, \overline{tar}) - \max\left(E(\overline{newref}, \overline{tar})\right)}{2md^3}\right) - 1\right);$$

$$V_b = \left(\sum_{u,v,w} R(u,v,w)u, \sum_{u,v,w} R(u,v,w)v, \sum_{u,v,w} R(u,v,w)w\right);$$

For a careful characterization of tracking accuracy, we defined two error components or measures of confidence: the absolute error *abserr* and the conservation error *conserr*. a*bserr* gives the error of resemblance to *absref*, as a measure of global variance or cumulative deviation from the model, while *conserr* shows the energy conservation at every frame, a measure of local variance.

$$abserr = E\left(\overline{absref}, \overline{tar}\right); conserr = E\left(\overline{ref}, \overline{tar}\right);$$

Both error measures should vary with the heart motion and the change in shape of ASD. For a correct tracking, the errors would become minimal at the same moment of the heat cycle. The errors are in percentage and normalized between 0 and 100, where 0 error corresponds to the perfect match.

3. OPTIMIZATION

Real-time tracking of ASD requires both an optimization of the memory management and an efficient scheme to compute the energy function E. E is the most time consuming operation in this algorithm due to both its numerical complexity and the large number of times it is called in the algorithm.

We took into account the large flexibility of the C/C++ language to limit memory allocations and benefit from the cache memory speed. Temporary objects have been reused as much as possible and frequent functions, such as the computation of the energy function, directly inlined in the code. Loops have been implemented using pointer arithmetic in order to suppress the cost of the multiplication required for random memory access.

Significant speed improvements have also been obtained by optimizing the computation the energy function $E(newref, tar)$, which can be rewritten as

$$E(\overline{newref}, \overline{tar}) = \frac{1}{n}\sum_i f\left(\ln \frac{\overline{newref}_i}{\overline{tar}_i}\right);$$

with

$$f(x) = x - \ln(e^{2x} + 1);$$

Evaluating the function f is time consuming due to the computation of the logarithmic and exponential functions. However, this process can be accelerated using the following scheme: f is an even function of x and is asymptotically equal *to* $f(x) \sim -|x|$ for large values of $|x|$; the relative error $(f(x)+|x|)/|x|$ is lower than 1% for $|x|>2$. Therefore, we pre-computed and stored the values of f for $x \in [0;2]$ and used the asymptotical expression for larger values, which ensures that arbitrarily large values of x would be accurately taken into account.

4. RESULTS

To test the tracking algorithms, we used a database of eight 4D time sequences of porcine beating hearts with artificially created ASD. While available clinical data is sparse, using animal data, we ensured a larger database for our study. Another strong incentive to use animal data is the need for animal studies to design surgery.

The ASDs were created solely under real-time 3D echorcardiographic guidance by balloon atrial septectomy. The experimental protocol was approved by the Children's Hospital Boston Institutional Animal Care and Use Committee. The size of the septal defects varied between 4.8 and 6.5 mm. All the US data were acquired in-vivo with a Sonos 7500 Live 3D Echo scanner (Philips Medical Systems, Andover, MA, USA). The image size is 80x80x176. The time of acquisition was of 2s/case at a frame rate of 25 volumes/s.

Figure 2 shows the entire 3D US volume with the position of the block marked. We show results at frames 1, 25 and 50. Each block shown in Figure 3 is a 3D entity visualized from the right atrium looking into the left atrium (from above the block) using a 3D renderer and semi-transparency. In this particular view, a well-tracked ASD will appear as a black hole in the middle of the block, where the surrounding tissue is part of the septum. The rows present the absolute reference in frame 1 and tracking results after 10, 20, 30, 40 and 50 frames (50 frames correspond to 2s).

Estimating *abserr* and *conserr* at every frame in a typical ASD 4D volume, we obtained the results shown in Figure 4. Our data are ungated, but Figure 4 shows repeatability in the pattern of error variation in time. Under the procedure, a typical porcine heart beats at 70 beat/min. For a data set of 50 frames (2s), the heart goes through approximately two and a half cardiac cycles. *abserr* becomes maximal at times when the ASD exhibits extreme changes of shape in a repetitive way with the heart cycle. *conserr* shows peaks at sudden movements of the heart septum related to the pumping of the heart. The errors also show a small increase in time, a cumulative error that could be corrected using gating information on the repetitiveness of the heart cycle. *abserr* has a mean value of 5.55 and a standard deviation of 2.32. *conserr* has a mean value of 3.34 and a standard deviation of 1.64.

The 3D cyclic motion of the block is further observed in Figure 5. The maximum computed displacement appears on the z-axis, due to the heart contraction/dilation, and is of approximately 10 voxels. The x and y displacements from one cycle to the next are partly due to the free-hand probe motion.

Using the described optimization scheme, the tracking algorithm becomes much faster. Previously, we reported results using a Matlab 7 (MathWorks, Inc.) on a Pentium IV machine with 1GB RAM and 2.40 GHz processor. The computational speed for an image size of 80x80x176 and a block size of 18x18x11 was of 3 s/frame [5]. With the modified block flow algorithm, we increased the speed to 2 Hz, or 5Hz on a more performant architecture (Intel Core2Duo T7200, 2GHz, 4MB L2 Cache, 667 MHz FSB, 667MHz DDR2 RAM). The results obtained with our optimized scheme in C++ achieved 26 Hz (US real-time) on the Pentium IV machine, and 41 Hz on the Core2Duo Processor.

5. DISCUSSION

We presented a modified block flow technique, optimized for the real-time tracking of ASD to assists in minimally invasive beating heart surgery. The algorithm combines the probability-based velocity computation for an entire block with template matching.

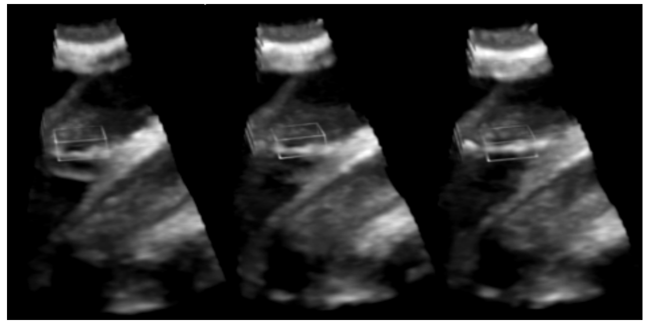

Figure 2: Tracking results in 3D volume. From left to right, the columns show the entire US volume with the 3D block delineated at frames 1, 25 and 50.

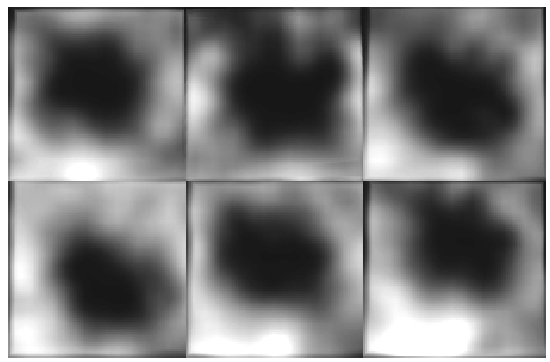

Figure 3: Tracking results by block. From left to right and top to bottom, the columns show 3D blocks (seen from the right atrium into the left atrium) at frames 1, 10, 20, 30, 40 and 50.

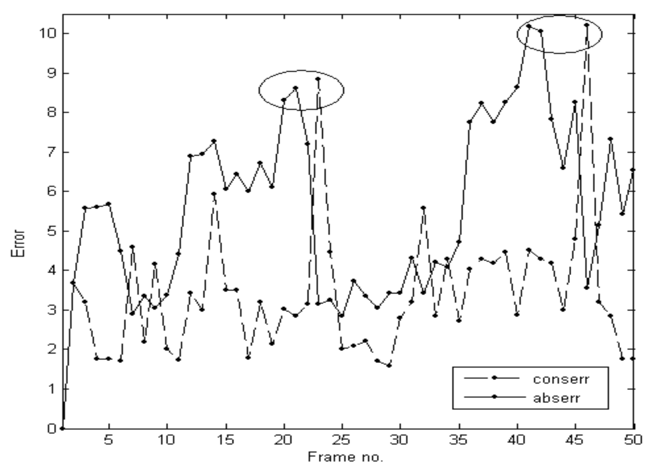

Figure 4: The evolution in time of the absolute and conservation errors. Although data are ungated, each error measure has two peaks, which are temporally related to each other, as shown by the two ellipses.

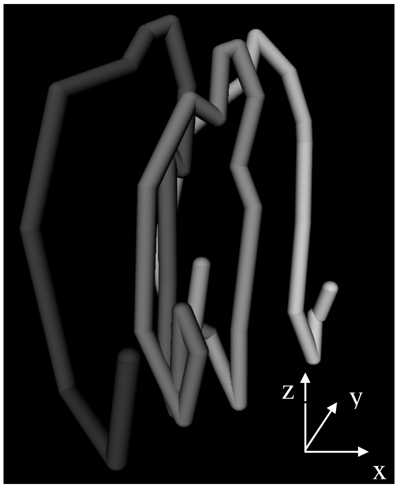

Figure 5: The 3D motion of the block in a porcine case. Temporal frames start at dark gray and evolve to lighter shades of gray.

We first normalized the intensities to reduce the effect of noise change and angular reflections from frame to frame. We used a Rayleigh noise model in the energy function. Although we did not smooth the data, the pre-processing of the commercial ultrasound machines may alter the noise distribution. Our assumption led to robust results, but other noise models may be studied.

Our tracking method obtained robust results on in-vivo animal data. After visual validation by medical experts, our results have sufficient tracking accuracy to guide the placement of the surgical patch over the ASD. The method was not sensitive to the size of ASD, the change in resolution or the motion of the US probe. An interesting observation was the cyclic evolution of errors in ungated cardiac data. We will investigate the use of the cardiac cycle for predictive estimation to minimize tracking errors.

The ideal speed of tracking should be equal to that of the US frame rate at 25 frames/s. Our optimized tracking method achieved the desired speed on an average Pentium IV processor and 41 Hz on a more performant Core2Duo processor. The residual processing time can be used for additional computational and accuracy features, as well as visualization and instrument control.

Other sources of errors, such as free-hand movements will be considered. We will include a larger study on clinical images acquired over more heart cycles. For the intricate process of assisting surgical interventions on beating heart, real-time ASD tracking will be combined with real-time instrument tracking [6]. While the ASD tracking is performed on CPU, the instrument tracking uses a Graphical Processing Unit (GPU). GPU algorithm implementations would be advantageous mainly for algorithms using projections and convolutions, which our application does not use. Hence, the real-time tracking methods for ASD and instruments can be ran on separate computational resources and combined in a complex real-time tracking tool.

ACKNOWLEDGEMENT

This work is funded by the National Institutes of Health under grant NIH R01 HL073647-01.

REFERENCES

[1] L.N. Benson, and R.M. Freedom "Atrial Septal Defect". In: R.M. Freedom, L.N. Benson, and J.F. Smallborn (Eds.), *Neonatal Heart Disease*, Springer, London, pp. 633-644, 1992.

[2] D. Boukerroui, J.A. Noble, and M. Brady, "Velocity Estimation in Ultrasound Images: a Block Matching Approach", I*nformation Processing in Medical Imaging* (IPMI 2003), pp. 586-598, 2003.

[3] J.W. Cannon, J.A. Stoll, I.S. Salgo, H.B. Knowles, R.D. Howe, P.E. Dupont, G.R. Marx, and P.J. del Nido, "Real Time 3-Dimensional Ultrasound for Guiding Surgical Tasks", *Computer Aided Surgery*, Vol. 8, pp. 82-90, 2003.

[4] S.W. Downing, W.R. Herzog Jr., M.C. McElroy, and T.B. Gilbert, "Feasibility of Off-pump ASD Closure using Real-time 3-D Echocardiography", *Heart Surgery Forum*, Vol. 5(2), pp. 96-99, 2002.

[5] M.G. Linguraru, N.V. Vasilyev, P.J. del Nido, and R.D. Howe, "Atrial Septal Defect Tracking in 3D Cardiac Ultrasound". In: R. Larsen, M. Nielsen, and J. Sporring (Eds.), *Medical Image Computing and Computer-Assisted Interventio*n – MICCAI 2006, Lecture Notes in Computer Science, Vol. 4190, Springer, New York, pp. 596-603, 2006.

[6] P.M. Novotny, J.A. Stoll, N.V. Vasilyev, P.J. del Nido, P.E. Dupont, and R.D. Howe, "GPU Based Real-Time Instrument Tracking with Three Dimensional Ultrasound". In: R. Larsen, M. Nielsen, and J. Sporring (Eds.), *Medical Image Computing and Computer-Assisted Interventio*n – MICCAI 2006, Lecture Notes in Computer Science, Vol. 4190, Springer, New York, pp. 58-65, 2006.

[7] A. Singh, and P. Allen, "Image-flow Computation: an Estimation-theoretic Framework and a Unified Perspective", *CVGIP: Image Understanding*, Vol. 65(2), pp. 152-177, 1992.

[8] Y. Suematsu, J.F. Martinez, B.K. Wolf, G.R. Marx, J.A. Stoll, P.E. DuPont, R.D. Howe, J.K. Triedman, and P.J. del Nido, "Three-dimensional Echo-guided Beating Heart Surgery without Cardiopulmonary Bypass: Atrial Septal Defect Closure in a Swine Model", *Journal Thoracic Cardiovascular Surgery*, Vol. 130(5), pp. 1348-1357, 2005.